

# Proper orthogonal decomposition approach and error estimation of mixed finite element methods for the tropical Pacific Ocean reduced gravity model

Zhendong Luo <sup>a</sup>, Jiang Zhu <sup>b</sup>, Ruiwen Wang <sup>b</sup>, I.M. Navon <sup>c,\*</sup>

<sup>a</sup> School of Science, Beijing Jiaotong University, Beijing 100044, PR China

<sup>b</sup> Institute of Atmospheric Physics, Chinese Academy of Sciences, Beijing 100029, PR China

<sup>c</sup> School of Computational Science and Department of Mathematics, Florida State University, Dirac Science Library Building, #483, Tallahassee, FL 32306-4120, USA

Received 19 January 2007; received in revised form 9 March 2007; accepted 12 April 2007

Available online 8 May 2007

## Abstract

In this paper, the tropical Pacific Ocean reduced gravity model is studied using the proper orthogonal decomposition (POD) technique of mixed finite element (MFE) method and an error estimate of POD approximate solution based on MFE method is derived. POD is a model reduction technique for the simulation of physical processes governed by partial differential equations, e.g., fluid flows or other complex flow phenomena. It is shown by numerical examples that the error between POD approximate solution and reference solution is consistent with theoretical results, thus validating the feasibility and efficiency of POD method.

© 2007 Elsevier B.V. All rights reserved.

**Keywords:** Proper orthogonal decomposition technique; Mixed finite element method; Error estimate; Numerical simulation

## 1. Introduction

The variability of fluid flow and fluid total layer thickness over tropical oceans is an important question in studies of climate change and air–sea interaction. However, the accurate assessment of fluid flow and fluid total layer thickness is greatly limited due to the lack of direct measurements and the insufficient knowledge of air–sea exchange processes. The tropical Pacific Ocean reduced gravity model is a useful model to simulate fluid flow and fluid total layer thickness over tropical Pacific Ocean and it has been extensively applied to studying the ocean dynamics in tropical regions (see Cane [1] and Seager et al. [2]). The model consists of two layers above the thermocline with the same constant density. The ocean below the ther-

mocline, with a higher density, is assumed to be sufficiently deep so that its velocity vanishes (Fig. 1). The upper of the two active layers is a fixed-depth surface layer in which the thermodynamics are included. The surface layer communicates with the lower active layer through entrainment/detrainment at their interface and through frictional horizontal shearing. We assume that there is no density difference across the base of the surface layer; that is, the surface layer is treated as part of the upper layer.

Following Seager et al. [2], the equations for the depth-averaged currents are

$$\begin{cases} \frac{\partial u}{\partial t} - fv = -g' \frac{\partial h}{\partial x} + \frac{\tau^x}{\rho_0 H} + A \nabla^2 u, & (x, y, t) \in \Omega \times (0, T_1), \\ \frac{\partial v}{\partial t} + fu = -g' \frac{\partial h}{\partial y} + \frac{\tau^y}{\rho_0 H} + A \nabla^2 v, & (x, y, t) \in \Omega \times (0, T_1), \\ \frac{\partial h}{\partial t} + H \left( \frac{\partial u}{\partial x} + \frac{\partial v}{\partial y} \right) = 0, & (x, y, t) \in \Omega \times (0, T_1), \end{cases} \quad (1.1)$$

with the boundary conditions

\* Corresponding author. Tel.: +1 850 644 6560; fax: +1 850 644 0098.  
E-mail address: [navon@scs.fsu.edu](mailto:navon@scs.fsu.edu) (I.M. Navon).

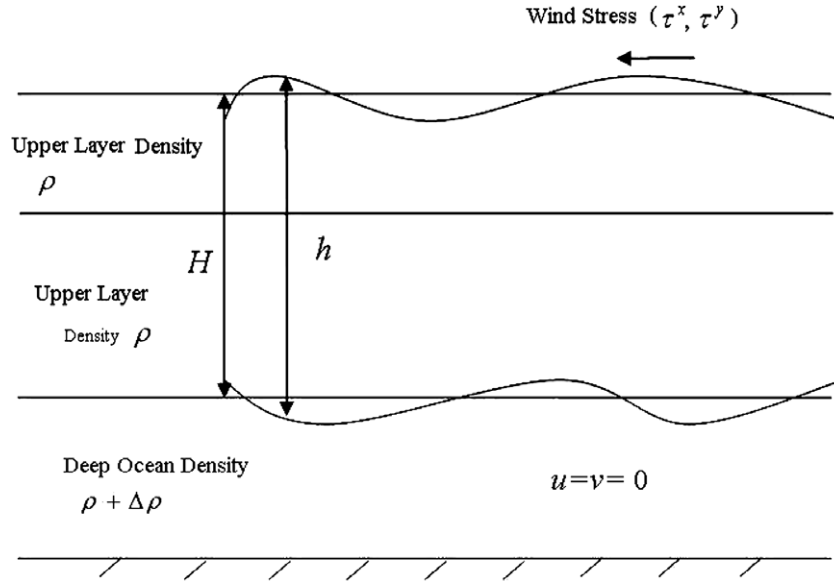


Fig. 1. Ocean depth.

$$\begin{cases} u(x, y, t)|_{\partial\Omega} = u_b(x, y, t), & (x, y, t) \in \partial\Omega \times (0, T_1), \\ v(x, y, t)|_{\partial\Omega} = v_b(x, y, t), & (x, y, t) \in \partial\Omega \times (0, T_1), \\ h(x, y, t)|_{\partial\Omega} = h_b(x, y, t), & (x, y, t) \in \partial\Omega \times (0, T_1), \end{cases} \quad (1.2)$$

and initial condition

$$\begin{aligned} u(x, y, 0) &= u^0(x, y), & v(x, y, 0) &= v^0(x, y), \\ h(x, y, 0) &= h^0(x, y), & (x, y) &\in \Omega, \end{aligned} \quad (1.3)$$

where  $(u, v)$  is the horizontal velocity of the depth-averaged currents;  $h$  the total layer thickness;  $f$  the Coriolis force;  $H$  the mean depth of the layer (constant);  $\rho_0$  the density of water;  $g'$  the reduced gravity; and  $A$  the horizontal eddy viscosity coefficient. The wind stress vector  $(\tau^x, \tau^y)$  is calculated by the aerodynamic bulk formula

$$(\tau^x, \tau^y) = \rho_a C_D \sqrt{U_{\text{wind}}^2 + V_{\text{wind}}^2} (U_{\text{wind}}, V_{\text{wind}}).$$

Here  $\rho_a$  is the density of the air;  $C_D$  the wind stress drag coefficient;  $(U_{\text{wind}}, V_{\text{wind}})$  the wind velocity vector;  $\Omega$  denotes the two dimensional rectangular domain, which is chosen from 30°S to 30°N in latitude and from 130°E to 70°W in longitude;  $u_b(x, y, t)$ ,  $v_b(x, y, t)$ ,  $h_b(x, y, t)$ ,  $u^0(x, y)$ ,  $v^0(x, y)$ , and  $h^0(x, y)$  are all given functions.

The seasonal net surface heat flux over tropical oceans has been only simulated with Eqs. (1.1)–(1.3) augmented by a thermodynamics equation as in Yu and O'Brien (see [3]). However, since the computational field over the tropical Pacific Ocean is very extensive, in order to obtain high resolution numerical solutions of fluid flow and fluid total layer thickness over tropical oceans, gridding points must be taken with enough density, thus requiring a large number of degree of freedom rendering computing very difficult. Thus, an important problem is how to simplify the computational load and save time-consuming calculations and resource demands in the actual computational process in a sense that guarantees a sufficiently accurate numerical

solution. Proper orthogonal decomposition (POD) is also known as Karhunen–Loève expansions in signal processing and pattern recognition (see [4]), principal component analysis in statistics (see [5]), and the method of empirical orthogonal functions in geophysical fluid dynamics (see [6,7]) or meteorology (see [8]). The POD technique offers adequate approximation to represent fluid flow with a reduced number of degrees of freedom, i.e., with lower dimensional models (see [9]) in order to simplify the computation and save CPU and memory requirements. POD has also found widespread applications in problems related to the approximation of large-scale models. Although the basic properties of POD method are well established and studies have been conducted to evaluate the suitability of this technique for various fluid flows (see [10–12]), its applicability and limitations for actual fluid flow and fluid total layer thickness over the tropical Pacific Ocean are not well documented.

The POD method mainly provides a useful tool for efficiently approximating a large amount of data. The method essentially provides an orthogonal basis for representing the given data in a certain least squares optimal sense, that is, it provides a way to find optimal lower dimensional approximations of the given data. In addition to being optimal in a least squares sense, POD has the property that it uses a modal decomposition that is completely data dependent and does not assume any prior knowledge of the process used to generate the data. This property is advantageous in situations where *a priori* knowledge of the underlying process is insufficient to warrant a certain choice of basis. Combined with the Galerkin projection procedure, POD provides a powerful method for generating lower dimensional models of dynamical systems that have a very large or even infinite dimensional phase space. The fact that this method always searches for linear (or affine) subspaces instead of curved submanifolds makes it

computationally tractable. In many cases, the behavior of a dynamic system is governed by characteristics or related structures, even though the ensemble is formed by a large number of different instantaneous solutions. POD method can capture these temporal and spatial structures by applying a statistical analysis to the ensemble of data.

In fluid dynamics, Lumley first employed the POD technique to capture the large eddy coherent structures in a turbulent boundary layer (see [13]); this technique was further extended in [14], where a link between the turbulent structure and dynamics of a chaotic system was investigated. In Holmes et al. [9], the overall properties of POD are reviewed and extended to widen the applicability of the method. The method of snapshots was introduced by Sirovich [15], and is widely used in applications to reduce the order of POD eigenvalue problem. Examples of these are optimal flow control problems [16–18] and turbulence [9,13,14,19,20].

In many applications, the POD method is used to generate basis functions for a reduced order model (ROM), which can simplify and provide quicker assessment of the major features of the fluid dynamics for the purpose of flow control demonstrated by Kurdila et al. [18] or design optimization shown by Ly et al. [17]. This application is used in a variety of other physical applications, such as in [17], which demonstrates an effective use of POD for a chemical vapor deposition (CVD) reactor.

In [21], while the tropical Pacific Ocean reduced gravity model is preliminarily dealt with POD method, an exact theoretical analysis was not carried out, in particular an error estimate of the POD approximate solution was not as yet derived. The objective of this paper is to investigate in depth to what extent can POD be successfully used to approximate a mixed finite element (MFE) solution for the tropical Pacific Ocean reduced gravity model. In particular, we aim to provide an error estimate of the approximate MFE solution, so that one could determine the number of required eigenmodes. Some numerical examples are provided for validating the proposed theory.

## 2. Outline of proper orthogonal decomposition technique

The essential problem of POD is to identify the underlying, coherent structures of a collected ensemble of data. POD entails finding the optimal bases and constructing a model of reduced dimension to approximate the original ensemble. Originally, POD was used as a data representation technique. For model reduction of dynamical systems, POD may be used on data points derived from system trajectories obtained via experiments, numerical simulations, or analytical derivations.

### 2.1. Continuous case

Let  $U_i(\vec{x})$  ( $i = 1, 2, \dots, n$ ) denote the set of  $n$  observations (also called snapshots) of some physical process taken

at position  $\vec{x} = (x, y)$ . The average of the ensemble of snapshots is given by

$$\bar{U} = \langle U \rangle = \frac{1}{n} \sum_{i=1}^n U_i(\vec{x}). \quad (2.1)$$

We form new ensemble by focusing on deviations from the mean as follows:

$$V_i = U_i - \bar{U}. \quad (2.2)$$

We wish to find an optimal compressed description of the sequence of data (2.2). One description of the process is a series expansion in terms of a set of basis functions. Intuitively, the basis functions should in some sense be representative of the members of the ensemble. Such a coordinate system, which possesses several optimality properties (to be discussed in the sequel), is provided by the Karhunen–Loève expansion (see [4]), where the basis functions are  $\Phi$ , in fact, admixtures of the snapshots and are given by

$$\Phi = \sum_{i=1}^n a_i V_i(\vec{x}), \quad (2.3)$$

where the coefficients  $a_i$  are to be determined such that  $\Phi$  given by (2.3) will most resemble the ensemble  $\{V_i(\vec{x})\}_{i=1}^n$ . More specifically, POD seeks a function  $\Phi$  such that

$$\frac{1}{n} \sum_{i=1}^n |(V_i, \Phi)|^2, \quad (2.4)$$

subject to

$$(\Phi, \Phi) = \|\Phi\|_0^2 = 1, \quad (2.5)$$

is minimized, where  $(\cdot, \cdot)$  and  $\|\cdot\|_0$  denote the usual  $L^2$ -inner product and  $L^2$ -norm, respectively (see Section 3.1).

It follows that (see, e.g. [22]) the basis functions are the eigenfunctions of the integral equation

$$\int_{\Omega} C(\vec{x}, \vec{x}') \Phi(\vec{x}') d\vec{x}' = \lambda \Phi(\vec{x}), \quad (2.6)$$

where the covariance kernel is given by

$$C(\vec{x}, \vec{x}') = \frac{1}{n} \sum_{i=1}^n V_i(\vec{x}) V_i(\vec{x}'). \quad (2.7)$$

Substituting (2.3) into (2.6) yields the following eigenvalue problem:

$$\sum_{j=1}^n L_{ij} a_j = \lambda a_i, \quad i = 1, 2, \dots, n, \quad (2.8)$$

where  $L_{ij} = \frac{1}{n} (V_i, V_j)$ ,  $L = (L_{ij})_{n \times n}$  is a symmetric and non-negative matrix. Thus we see that our problem amounts to solving for the eigenvectors of an  $n \times n$  matrix where  $n$  is the size of the ensemble of snapshots. Straightforward calculation (see also [22]) shows that the cost functional

$$\frac{1}{n} \sum_{i=1}^n |(V_i, \Phi)|^2 = (\lambda \Phi, \Phi) = \lambda$$

is maximized when the coefficients  $a_i$  ( $i = 1, 2, \dots, n$ ) of (2.8) are the elements of the eigenvector corresponding to the largest eigenvalue of  $L$ .

### 2.2. Discrete case

Alternatively, we also can consider the discrete Karhunen–Loève expansion to find an optimal representation of the ensemble of snapshots. In general, each sample of snapshots  $U_i(\vec{x})$  (defined on a set of  $m$  nodal points  $\vec{x}$ ) can be expressed as a  $m$  dimensional vector  $\vec{u}_i$  as follows:

$$\vec{u}_i = (u_{i1}, u_{i2}, \dots, u_{im})^T, \quad (2.9)$$

where  $u_{ij}$  denotes the  $j$ th component of the vector  $\vec{u}_i$  ( $i = 1, 2, \dots, n$ ). The mean of vector is given by

$$\bar{u}_k = \sum_{i=1}^n u_{ik}, \quad k = 1, 2, \dots, m. \quad (2.10)$$

We also can form a new ensemble by focusing on deviations from the mean value as follows:

$$v_{ik} = u_{ik} - \bar{u}_k, \quad k = 1, 2, \dots, m. \quad (2.11)$$

Let the matrix  $A$  denote the new ensemble

$$A = \begin{pmatrix} v_{11} & v_{21} & \cdots & v_{n1} \\ v_{12} & v_{22} & \cdots & v_{n2} \\ \vdots & \vdots & \vdots & \vdots \\ v_{1m} & v_{2m} & \cdots & v_{nm} \end{pmatrix}_{m \times n},$$

where the discrete covariance matrix of the ensemble may be written as

$$AA^T \vec{y}_k = \lambda_k \vec{y}_k, \quad k = 1, 2, \dots, m, \quad \vec{y}_k \in R^{m \times m}. \quad (2.12)$$

Thus, to compute the POD mode, one must solve a  $m \times m$  eigenvalue problem. For a discretization of an ocean problem, the dimension often exceeds  $10^4$ , so that a direct solution of this eigenvalue problem is often not feasible. We can transform the eigenvalue problem into an  $n \times n$  eigenvalue problem (see [23]). In the method of snapshots, one then solves the  $n \times n$  eigenvalue problem

$$A^T A \vec{w}_k = \lambda_k \vec{w}_k, \quad k = 1, 2, \dots, n, \quad \vec{w}_k \in R^{n \times n}, \quad (2.13)$$

where the nonzero eigenvalues  $\lambda_k$  ( $1 \leq k \leq n$ ) are the same in (2.12). The eigenvectors may be chosen to be orthonormal, and the POD modes are given by  $\vec{\phi}_k = A \vec{w}_k / \sqrt{\lambda_k}$ . In matrix form, with  $\Phi = (\vec{\phi}_1, \vec{\phi}_2, \dots, \vec{\phi}_n)$ , and  $W = (\vec{w}_1, \vec{w}_2, \dots, \vec{w}_n)$ , this becomes  $\Phi = AW$ .

The eigenvalue problem (2.13) is more efficient than the  $m \times m$  eigenvalue problem (2.12) when the number of snapshots  $n$  is much smaller than the number of states  $m$ .

### 3. POD technique and error estimate of MFE method for tropical Pacific Ocean reduced gravity model

In this section, we apply the POD technique and MFE method to the upper tropical Pacific Ocean model

described in Section 1. This method provides a systematic way of creating a reduced basis space using the state of the system at different time instances. As in the general reduced order basis methods, the states could come from full order numerical computations (also obtained from system trajectories obtained via experiments, or by analytical derivations). Here, we apply the MFE methods to the upper tropical Pacific Ocean model for obtaining a full order numerical solution, then apply the POD technique to reconstruct the approximate solution and approximate the solution of the reduced model. Finally, we compare the error of the accurate solution with that of the approximate solution.

#### 3.1. MFE method for the tropical Pacific Ocean reduced gravity model

The Sobolev spaces along with their properties used in this context are standard (cf. Ref. [24]). For example, for bounded domain  $\Omega$ , we denote by  $H^m(\Omega)$  ( $m \geq 0$ ) and  $L^2(\Omega) = H^0(\Omega)$  the usual Sobolev spaces equipped with the semi-norm and the norm, respectively,

$$|v|_{m,\Omega} = \left\{ \sum_{|\alpha|=m} \int_{\Omega} |D^{\alpha} v|^2 dx dy \right\}^{1/2} \quad \forall v \in H^m(\Omega),$$

$$\|v\|_{m,\Omega} = \left\{ \sum_{i=0}^m |v|_{i,\Omega}^2 \right\}^{1/2} \quad \forall v \in H^m(\Omega),$$

where  $\alpha = (\alpha_1, \alpha_2)$ ,  $\alpha_1$  and  $\alpha_2$  are tow nonnegative integers, and  $|\alpha| = \alpha_1 + \alpha_2$ . Especially, the subspace  $H_0^1(\Omega)$  of  $H^1(\Omega)$  is denoted by

$$H_0^1(\Omega) = \{v \in H^1(\Omega); u|_{\partial\Omega} = 0\}.$$

Note that  $\|\cdot\|_1$  is equivalent to  $|\cdot|_1$  in  $H_0^1(\Omega)$ . Let  $L_0^2(\Omega) = \{q \in L^2(\Omega); \int_{\Omega} q dx dy = 0\}$ , which is the subspace of  $L^2(\Omega)$ . For the sake of convenience, we consider the mixed variational formulation for (1.1) with the boundary conditions

$$u(x, y, t)|_{\partial\Omega} = 0, \quad v(x, y, t)|_{\partial\Omega} = 0, \quad h(x, y, t)|_{\partial\Omega} = 0, \\ 0 \leq t \leq t_1.$$

Therefore, the variational form for the tropical Pacific Ocean reduced gravity model can be written as:

**Problem (I).** Find  $(u, v, h) \in H_0^1(\Omega) \times H_0^1(\Omega) \times L_0^2(\Omega)$  such that

$$\begin{cases} (u_t, \varphi) - f(v, \varphi) - g'(h, \varphi_x) + A(\nabla u, \nabla \varphi) = (f_1, \varphi) \\ \quad \forall \varphi \in H_0^1(\Omega), \\ (v_t, \psi) + f(u, \psi) - g'(h, \psi_y) + A(\nabla v, \nabla \psi) = (f_2, \psi) \\ \quad \forall \psi \in H_0^1(\Omega), \\ (h_t, q) + H(u_x + v_y, q) = 0 \quad \forall q \in L_0^2(\Omega), \\ u(x, y, 0) = u^0(x, y), v(x, y, 0) = v^0(x, y), h(x, y, 0) \\ = h^0(x, y), \quad (x, y) \in \Omega, \end{cases}$$

where  $f_1 = \tau^x/(\rho_0 H)$  and  $f_2 = \tau^y/(\rho_0 H)$ . Using the same as approach in Ref. [25], we could check that **Problem (I)** has a unique solution.

In order to find the numerical solution for **Problem (I)**, it is necessary to discretize **Problem (I)**. We introduce a finite element approximation for the spatial variable and finite difference scheme for the time derivative. Let  $\mathfrak{T}_h$  be a uniform regular triangulation of  $\bar{\Omega}$  (here  $\Omega$  denotes the two dimensional rectangular domain, which is chosen from 30°S to 30°N in latitude and from 130°E to 70°W in longitude in actual computation), i.e., for any  $K \in \mathfrak{T}_h$ , put  $\bar{h}_K = \text{diam}\{K\}$ ,  $\bar{h} = \max_{K \in \mathfrak{T}_h} \{\bar{h}_K\}$ , then  $c\bar{h} \leq \bar{h}_K \leq c_1\bar{h}$ . Denote the time step increment by  $k = T_1/N$  ( $T_1$  being the total time) and MFE approximation of  $(u, v, h)$  by  $(u_h^l, v_h^l, h_h^l) = (u_h(x, y, t_l), v_h(x, y, t_l), h_h(x, y, t_l))$ ,  $t_l = lk$  ( $0 \leq l \leq N$ ). Define the finite element subspaces of  $H_0^1(\Omega)$  and  $L_0^2(\Omega)$  as follows, respectively,

$$\begin{cases} X_h = \{\varphi_h \in H_0^1(\Omega); \varphi_h|_K \in P_m(K) \quad \forall K \in \mathfrak{T}_h\}, \\ L_h = \{q_h \in L_0^2(\Omega); q_h|_K \in P_{m-1}(K) \quad \forall K \in \mathfrak{T}_h\}, \end{cases}$$

where  $m \geq 1$  is integer,  $P_m(K)$  polynomial subspace of degrees  $\leq m$  on  $K$ . Then, the fully discrete formulation for **Problem (I)** can be written as:

**Problem (II).** Find  $(u_h^l, v_h^l, h_h^l) \in X_h \times X_h \times L_h$  ( $l = 1, 2, \dots, N$ ) such that

$$\begin{cases} (u_h^l, \varphi_h) - kf(v_h^l, \varphi_h) - kg'(h_h^l, \varphi_{hx}) + kA(\nabla u_h^l, \nabla \varphi_h) \\ \quad = k(f_1^l, \varphi_h) + (u_h^{l-1}, \varphi_h) \quad \forall \varphi_h \in X_h, \\ (v_h^l, \psi_h) + kf(u_h^l, \psi_h) - kg'(h_h, \psi_{hy}) + kA(\nabla v_h^l, \nabla \psi_h) \\ \quad = k(f_2^l, \psi_h) + (v_h^{l-1}, \psi_h) \quad \forall \psi_h \in X_h, \\ (h_h^l, q_h) + kH(u_{hx}^l + v_{hy}^l, q_h) = (h_h^{l-1}, q_h) \quad \forall q_h \in L_h, \\ l = 1, 2, \dots, N, \\ u_h^0 = u^0(x, y), \quad v_h^0 = v^0(x, y), \quad h_h^0 = h^0(x, y), \end{cases}$$

where  $f_1^l = f_1(t_l)$  and  $f_2^l = f_2(t_l)$ . Using the same as approach as in [26], we could check that **Problem (II)** has unique solution  $(u_h^l, v_h^l, h_h^l) \in X_h \times X_h \times L_h$ , and if solution  $(u, v, h) \in H^{m+1}(\Omega) \times H^{m+1}(\Omega) \times H^m(\Omega)$  of **Problem (I)**, the following error estimates hold:

$$\begin{cases} \|u(x, y, t_l) - u_h^l\|_0 + k^{1/2} \sum_{j=1}^l \|\nabla(u(x, y, t_l) - u_h^l)\|_0 \\ \leq c(\bar{h}^m + k), \\ \|v(x, y, t_l) - v_h^l\|_0 + k^{1/2} \sum_{j=1}^l \|\nabla(v(x, y, t_l) - v_h^l)\|_0 \\ \leq c(\bar{h}^m + k), \\ \|h(x, y, t_l) - h_h^l\|_0 \leq c(\bar{h}^m + k), \quad l = 1, 2, \dots, N, \end{cases} \quad (3.1)$$

where  $c$  is a constant independent of  $\bar{h}$  and  $k$ , but dependent of  $(u, v, h)$ .

### 3.2. POD technique for the tropical Pacific Ocean reduced gravity model

In the construction described above in Section 2, the number  $n$  may be large, depending on the complexity of the dynamics represented in the ‘‘snapshots’’. In general, one should take  $n$  sufficiently large so that the snapshots  $U_i(x, y)$  contain all the salient features of the dynamics being investigated. Thus, the POD basis functions  $\Phi_i$  ( $1 \leq i \leq n$ ), used with the original dynamics in a Galerkin procedure, offer the possibility of achieving a high fidelity model albeit with perhaps a dimension  $n$ .

To apply the POD techniques to the upper tropical Pacific Ocean model in Section 1, we first solve **Problem (II)** at  $N$  time steps and obtain the solutions  $(u_h^l, v_h^l, h_h^l)$  ( $l = 1, 2, \dots, N$ ) of velocity field and upper layer thickness at an increment of  $k = T_1/N$  (for example,  $T_1 = 1$  year) day for  $(x, y) \in \Omega$ . And then we choose  $n$  (for example,  $n = 5, 20$ , or 30, in general,  $n \ll N$ ) snapshots  $U_i(x, y) = (u_h^i, v_h^i, h_h^i)$  ( $i = 1, 2, \dots, n$ ) (which is useful and of interest for us) from  $N$  group of solutions  $(u_h^l, v_h^l, h_h^l)$  ( $1 \leq l \leq N$ ) for **Problem (II)**. These snapshots are discrete data over  $\Omega$ . Using (2.10), (2.11), and (2.13) yields covariance matrices  $A_u^T A_u, A_v^T A_v, A_h^T A_h$  associated with  $(u_h^i, v_h^i, h_h^i)$  ( $i = 1, 2, \dots, n$ ). Since those matrices are all nonnegative Hermitian matrices, they all have a complete set of orthogonal eigenvectors with the corresponding eigenvalues arranged in ascending order as  $\lambda_1^u \geq \lambda_2^u \geq \dots \geq \lambda_n^u \geq 0$ ,  $\lambda_1^v \geq \lambda_2^v \geq \dots \geq \lambda_n^v \geq 0$ , and  $\lambda_1^h \geq \lambda_2^h \geq \dots \geq \lambda_n^h \geq 0$ , respectively. Then we construct POD basis elements  $\Phi_i^u(x, y)$ ,  $\Phi_i^v(x, y)$ ,  $\Phi_i^h(x, y)$  such that

$$\begin{cases} X_u^{\text{POD}} = \text{span}\{\Phi_1^u(x, y), \Phi_2^u(x, y), \dots, \Phi_n^u(x, y)\}, \\ X_v^{\text{POD}} = \text{span}\{\Phi_1^v(x, y), \Phi_2^v(x, y), \dots, \Phi_n^v(x, y)\}, \\ X_h^{\text{POD}} = \text{span}\{\Phi_1^h(x, y), \Phi_2^h(x, y), \dots, \Phi_n^h(x, y)\}, \end{cases} \quad (3.2)$$

are defined as

$$\begin{aligned} \Phi_j^u(x, y) &= \sum_{i=1}^n a_{ui}^j u_h^i, & \Phi_j^v(x, y) &= \sum_{i=1}^n a_{vi}^j v_h^i, \\ \Phi_i^h(x, y) &= \sum_{j=1}^n a_{hi}^j h_h^j, \end{aligned} \quad (3.3)$$

where  $a_{ui}^j, a_{vi}^j, a_{hi}^j$  ( $1 \leq i \leq n$ ) are the components of the eigenvectors  $A_u V_u^j / \sqrt{\lambda_{uj}}, A_v V_v^j / \sqrt{\lambda_{vj}}, A_h V_h^j / \sqrt{\lambda_{hj}}$  corresponding to the eigenvalues  $\lambda_j^u, \lambda_j^v, \lambda_j^h$ , respectively.

For three groups of basic functions  $\Phi_i^u(x, y), \Phi_i^v(x, y), \Phi_i^h(x, y)$  ( $i = 1, 2, \dots, n$ ), put

$$\begin{cases} u_h^s = \bar{u}(x, y) + \sum_{j=1}^n \beta_j^u(t_s) \Phi_j^u(x, y), \\ v_h^s = \bar{v}(x, y) + \sum_{j=1}^n \beta_j^v(t_s) \Phi_j^v(x, y), \\ h_h^s = \bar{h}(x, y) + \sum_{j=1}^n \beta_j^h(t_s) \Phi_j^h(x, y), \quad s = 1, 2, \dots, \end{cases} \quad (3.4)$$

where  $\beta_j^u(t_s)$ ,  $\beta_j^v(t_s)$ , and  $\beta_j^h(t_s)$  ( $j = 1, 2, \dots, n$ ) are coefficients to determine;  $\bar{u}(x, y)$ ,  $\bar{v}(x, y)$ , and  $\bar{h}(x, y)$  are the mean values of  $(u_h^i, v_h^i, h_h^i)$  ( $i = 1, 2, \dots, n$ ), respectively. Note that, if  $s = i$  ( $1 \leq i \leq n$ ),  $(u_h^s, v_h^s, h_h^s)$  are the solutions for Problem (II). Since the scales in model variables and are not uniform, one may employ different modes to reconstruct the solutions. In order to reduce order for Problem (II), we apply the POD approximate solution

$$\begin{cases} u_{M_1}^s = \bar{u}(x, y) + \sum_{j=1}^{M_1} \beta_j^u(t_s) \Phi_j^u(x, y), \\ v_{M_1}^s = \bar{v}(x, y) + \sum_{j=1}^{M_1} \beta_j^v(t_s) \Phi_j^v(x, y), \\ h_{M_2}^s = \bar{h}(x, y) + \sum_{j=1}^{M_2} \beta_j^h(t_s) \Phi_j^h(x, y), \quad s = 1, 2, \dots, \end{cases} \quad (3.5)$$

where  $\beta_j^u(t_s)$  and  $\beta_j^v(t_s)$  ( $j = 1, 2, \dots, M_1$ ),  $\beta_j^h(t_s)$  ( $j = 1, 2, \dots, M_2$ ),  $\bar{u}(x, y)$ ,  $\bar{v}(x, y)$ , and  $\bar{h}(x, y)$  are the same as Eq. (3.4). Substituting the solutions of Problem (II) with (3.4) and (3.5), respectively, we could obtain the following equations, respectively.

**Problem (III).** Find  $(\beta_r^u(t_s), \beta_r^v(t_s), \beta_r^h(t_s))$  ( $r = 1, 2, \dots, n$ ) such that

$$\begin{cases} \beta_r^u(t_s) - kf \sum_{j=1}^n \beta_j^v(t_s) (\Phi_j^v, \Phi_r^u) - kg' \sum_{l=1}^n \beta_l^h(t_s) (\Phi_l^h, \Phi_{rx}^u) \\ + kA \sum_{i=1}^n \beta_i^u(t_s) (\nabla \Phi_i^u, \nabla \Phi_r^u) = k(f_1^s, \Phi_r^u) + \beta_r^u(t_{s-1}), \\ \beta_r^v(t_s) + kf \sum_{i=1}^n \beta_i^u(t_s) (\Phi_i^u, \Phi_r^v) - kg' \sum_{l=1}^n \beta_l^h(t_s) (\Phi_l^h, \Phi_{ry}^v) \\ + kA \sum_{j=1}^n \beta_j^v(t_s) (\nabla \Phi_j^v, \nabla \Phi_r^v) = k(f_2^s, \Phi_r^v) + \beta_r^v(t_{s-1}), \\ \beta_r^h(t_s) + kH \sum_{i=1}^n \beta_i^u(t_s) (\Phi_{ix}^u, \Phi_r^h) + kH \sum_{j=1}^n \beta_j^v(t_s) (\Phi_{jy}^v, \Phi_r^h) = \beta_r^h(t_{s-1}), \\ r = 1, 2, \dots, n, \quad s = 1, 2, \dots, \end{cases}$$

along with the initial condition

$$\begin{cases} \beta_r^u(0) = (u(x, y, 0) - \bar{u}(x, y), \Phi_r^u(x, y)), \\ \beta_r^v(0) = (v(x, y, 0) - \bar{v}(x, y), \Phi_r^v(x, y)), \\ \beta_r^h(0) = (h(x, y, 0) - \bar{h}(x, y), \Phi_r^h(x, y)), \quad 1 \leq r \leq n. \end{cases} \quad (3.6)$$

**Problem (IV).** Find  $(\beta_r^u(t_s), \beta_r^v(t_s), \beta_\ell^h(t_s))$  ( $r = 1, 2, \dots, M_1$ ,  $\ell = 1, 2, \dots, M_2$ ) such that

$$\begin{cases} \beta_r^u(t_s) - kf \sum_{j=1}^{M_1} \beta_j^v(t_s) (\Phi_j^v, \Phi_r^u) - kg' \sum_{l=1}^{M_2} \beta_l^h(t_s) (\Phi_l^h, \Phi_{rx}^u) \\ + kA \sum_{i=1}^{M_1} \beta_i^u(t_s) (\nabla \Phi_i^u, \nabla \Phi_r^u) = k(f_1^s, \Phi_r^u) + \beta_r^u(t_{s-1}), \\ r = 1, 2, \dots, M_1, \quad s = 1, 2, \dots, \\ \beta_r^v(t_s) + kf \sum_{i=1}^{M_1} \beta_i^u(t_s) (\Phi_i^u, \Phi_r^v) - kg' \sum_{l=1}^{M_2} \beta_l^h(t_s) (\Phi_l^h, \Phi_{ry}^v) \\ + kA \sum_{j=1}^{M_1} \beta_j^v(t_s) (\nabla \Phi_j^v, \nabla \Phi_r^v) = k(f_2^s, \Phi_r^v) + \beta_r^v(t_{s-1}), \\ r = 1, 2, \dots, M_1, \quad s = 1, 2, \dots, \\ \beta_\ell^h(t_s) + kH \sum_{i=1}^{M_1} \beta_i^u(t_s) (\Phi_{ix}^u, \Phi_\ell^h) + kH \sum_{j=1}^{M_1} \beta_j^v(t_s) (\Phi_{jy}^v, \Phi_\ell^h) = \beta_\ell^h(t_{s-1}), \\ \ell = 1, 2, \dots, M_2, \quad s = 1, 2, \dots, \end{cases}$$

along with the initial condition

$$\begin{cases} \beta_r^u(0) = (u(x, y, 0) - \bar{u}(x, y), \Phi_r^u(x, y)), \quad r = 1, 2, \dots, M_1, \\ \beta_r^v(0) = (v(x, y, 0) - \bar{v}(x, y), \Phi_r^v(x, y)), \quad r = 1, 2, \dots, M_1, \\ \beta_\ell^h(0) = (h(x, y, 0) - \bar{h}(x, y), \Phi_\ell^h(x, y)), \quad \ell = 1, 2, \dots, M_2. \end{cases} \quad (3.7)$$

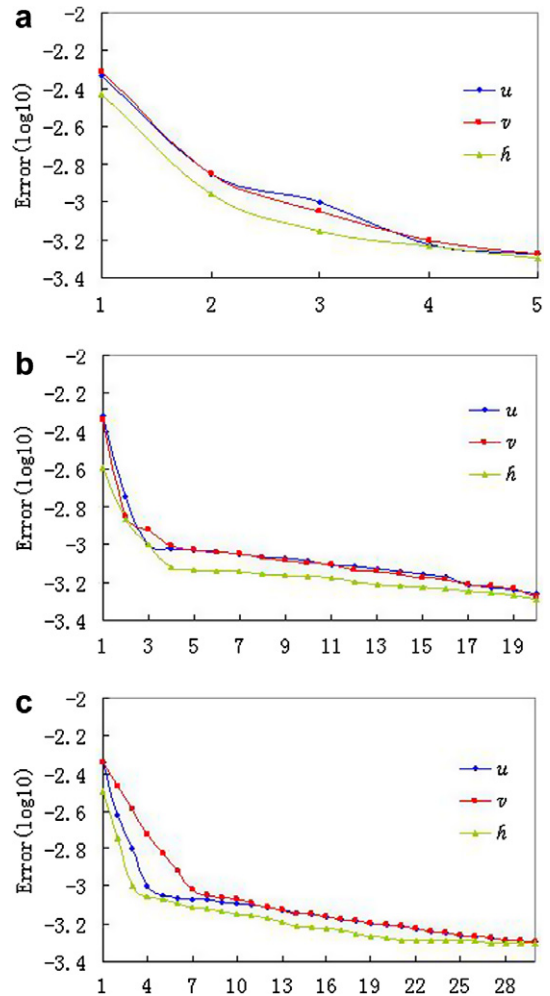


Fig. 2. Error of numerical solutions of different POD bases for 5, 20, and 30 snapshots. (a) 5 snapshots; (b) 20 snapshots; and (c) 30 snapshots.

There is the following error estimate between the solutions for Problem (III) and the solutions for Problem (IV), whose proof is provided in Appendix A.

**Theorem 1.** *If  $\max\{(\sum_{i=M_1+1}^n \lambda_i^u)^{1/2}, (\sum_{i=M_1+1}^n \lambda_i^v)^{1/2}\} \leq \hbar/c$  and  $k$  is sufficiently small, then the error estimate between the solutions for full basic Problem (II) and the solutions for the reduced order basic Problem (IV) is*

$$\|((u_h^s - u_{M_1}^s), (v_h^s - v_{M_1}^s), (h_h^s - h_{M_1}^s))\|_0 \leq \bar{C}_5 \left( \sum_{i=M_1+1}^n (\lambda_i^u + \lambda_i^v) + \sum_{i=M_2+1}^n \lambda_i^h \right),$$

where  $\bar{C}_5 = 3\bar{C}_4$  ( $\bar{C}_4$  see Appendix A) and  $s = 1, 2, \dots$

Combining (3.1) with Theorem 1 could yield in the following result.

**Theorem 2.** *If  $\max\{(\sum_{i=M_1+1}^n \lambda_i^u)^{1/2}, (\sum_{i=M_1+1}^n \lambda_i^v)^{1/2}\} \leq \hbar/c$  and  $k$  is sufficiently small, then the error estimate between the solutions for Problem (I) and the solutions for the reduced order basic Problem (IV) is*

$$\|((u(t_l) - u_{M_1}^l), (v(t_l) - v_{M_1}^l), (h(t_l) - h_{M_1}^l))\|_0 \leq c(\hbar^m + k) + \bar{C}_5 \left( \sum_{i=M_1+1}^n (\lambda_i^u + \lambda_i^v) + \sum_{i=M_2+1}^n \lambda_i^h \right),$$

$l = 1, 2, \dots, n.$

**Remark 1.** When one computes actual problems, one may obtain the ensemble of snapshots from physical system trajectories by drawing samples from experiments and interpolation (or data assimilation). For example, for weather forecast, one can use previous weather prediction results to construct the ensemble of snapshots, then restructure the POD basis for the ensemble of snapshots by Section 2, and finally combine it with a Galerkin projection to derive a reduced order dynamical system, i.e., one needs only to solve Problem (IV) which has only few degrees of freedom, but it is unnecessary to solve Problem (II). Thus, the forecast of future weather change can be quickly simulated, which is of major importance for actual real-life applications.

**Remark 2.** In general,  $c_0$  is a very small value so that  $\exp(kc_0n)$  approaches 1 in Theorem 1, and taking  $m = 1$  or 2 is sufficient in actual numerical simulations. Since our methods employ some MFE solutions  $(u_h^i, v_h^i, h_h^i)$  ( $i = 1, 2, \dots, n$ ) for Problem (II) as assistant analysis, the error estimates in Theorem 2 are correlated to the gridding scale  $\hbar$  and time step size  $k$ . However, using same argument as in Remark 1, the assistant  $(u_h^i, v_h^i, h_h^i)$  ( $i = 1, 2, \dots, n$ ) could be substituted with the interpolation functions of experimental and previous results, it is unnecessary to solve Problem (II), it is only necessary to directly solve Problem (IV) such that Theorem 1 is satisfied. Since Problem (IV) is

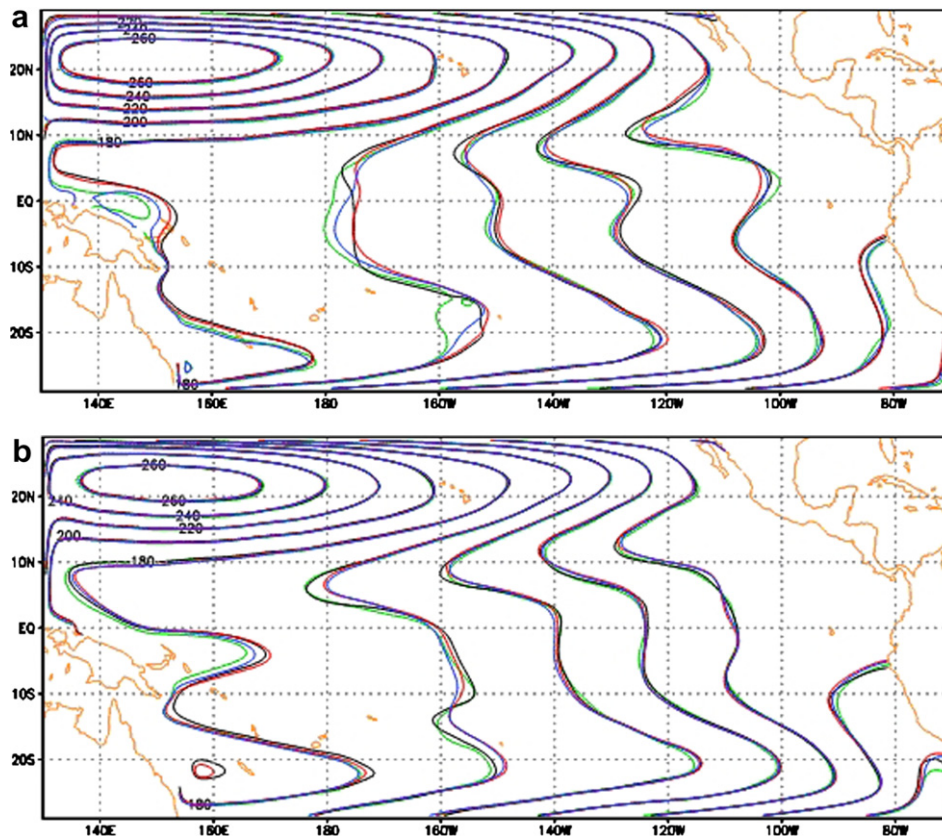


Fig. 3. Fluid total layer thickness for Problem (II) (black curve), 4 POD bases for 5 snapshots (green curve), 7 POD bases for 20 snapshots (red curve), and 7 POD bases for 30 snapshots for month of June (b) and December (d). (a) Case on June and (b) case on December.

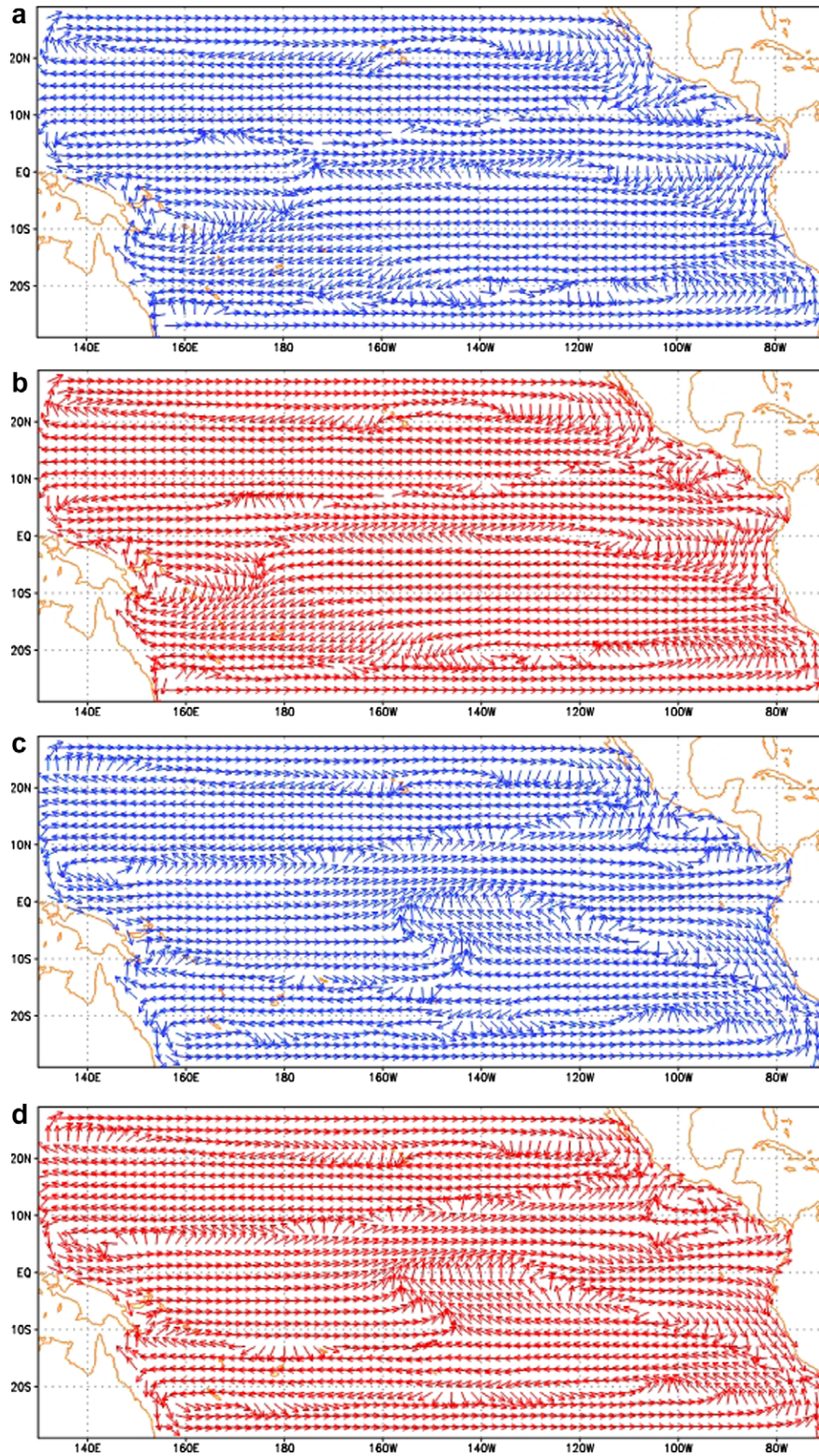


Fig. 4. Profiles of currents for Problem (II) (blue vector) for month of June (a) and December (c) and profiles of currents for Problem (IV) using 7 POD bases for 20 snapshots (red curve) for month of June (b) and December (d). (a) Currents for Problem (II) on June (b) currents for Problem (IV) on June (c) currents for Problem (II) on December (d) currents for Problem (IV) on December. (For interpretation of the references to colour in this figure legend, the reader is referred to the web version of this article.)

only dependent on  $M_1$  and  $M_2$ , and is independent of the gridding scale  $\bar{h}$  and time step size  $k$ , and, in general,  $M_1$  and  $M_2 \ll n$ , it is only necessary to solve **Problem (IV)** with very few freedom degrees.

#### 4. Some numerical examples

In this section, we present numerical computations related to the approaches presented in the previous paragraphs. In this study, we applied the model to the tropic Pacific Ocean domain  $\Omega$  (which is a domain 30°S–30°N, 130°E–70°W), using parameters values of  $f = 2(7.29E-5)\sin(x, y)$ ,  $H = 150$  m,  $\rho_0 = 1.2 \text{ kg m}^{-3}$ ,  $\rho_a = 1025 \text{ kg m}^{-3}$ ,  $g' = 3.7 \times 10^{-2}$ ,  $A = 750 \text{ m}^2 \text{ s}^{-1}$ , and  $C_D = 1.5 \times 10^{-3}$  for **Problem (I)**. This chosen model domain allows for all possible equatorially trapped waves to be excited by the applied wind forcing (see [3]). The no-normal flow and no-slip conditions are applied at these solid boundaries. We choose the uniform regular triangulation with  $\bar{h} = 0.5^\circ$  and the time mesh size to be  $k = 100$ s. The model is driven by the Florida State University (FSU) climatology monthly mean winds (cf. [27]), and the data are projected onto each time step by a linear interpolation and onto each grid point by a bilinear interpolation.

We choose 5, 20, and 30 group of solutions (i.e., snapshots) solving **Problem (II)** for 1 year. It is shown by computing that eigenvalues  $\lambda_{u4}$ ,  $\lambda_{v4}$ , and  $\lambda_{h4}$  are all less than  $10^{-3}$  if the number of snapshots is 5, while eigenvalues  $\lambda_{u8}$ ,  $\lambda_{v8}$ , and  $\lambda_{h8}$  are all less than  $10^{-3}$  if the number of snapshots is 20 and 30, which are consistent with the errors between numerical solutions obtained with a different number of POD optimal bases for **Problem (IV)** and solutions obtained with **Problem (II)**, where the red curve represents the error of fluid total layer thickness, the blue curve represents the error of fluid velocity in the longitude direction, and the green curve represents the error of fluid velocity in the latitude direction in Fig. 2.<sup>1</sup> It is shown by comparing results for **Problem (II)** and POD reduced model that the computational load for velocity vector and fluid total layer thickness with **Problem (IV)** is sizably reduced, and the error between them does not exceed  $10^{-3}$ . And the results of the error for the actual example are consistent with the theoretical results obtained by computing with **Theorem 2**. This also shows that finding the approximate solutions for the tropical Pacific Ocean reduced gravity model with **Problem (IV)** is computationally very effective.

We obtain the solution for fluid total layer thickness  $h$  depicted graphically in Fig. 3a and b, respectively, where the green curves represent numerical solution for 5 snapshots used 4 POD bases to solve reduced **Problem (IV)**, the red curves represent numerical solution for 20 snapshots used 7 POD bases to solve reduced **Problem (IV)**, the purple curves represent numerical solution for 20 snapshots used 7 POD bases to solve reduced **Problem (IV)**, and

the black curves represent the solutions solving **Problem (II)** on June and on December.

We also obtain the profiles of currents for fluid velocity  $(u, v)$  depicted graphically in Fig. 4b and d, respectively, for 20 snapshots using 7 POD bases to solve **Problem (IV)**, and Fig. 4a and c are, respectively, the solutions solving **Problem (II)** for June and for December.

These profiles demonstrate that the results of the numerical simulations coincide with both the theory and the actual cases. Especially, the POD reduced model **Problem (IV)** is a reduced method to apply the existing datum to simulating future phenomena, which has far fewer ( $2M_1 + M_2 \ll n$ ) degrees of freedom of **Problem (II)**. Therefore, the POD reduced method is very suitable for dealing with large-scale science engineering computations, and could simplify computing and reduces both CPU and memory requirements in the actual computational process in a sense that guarantees a sufficiently accurate numerical solution.

#### 5. Conclusions

In this paper, we have employed the POD and Galerkin techniques to study the reduced format for the tropical Pacific Ocean reduced gravity model and to reconstruct POD optimal orthogonal bases of ensembles of data which are compiled from transient solutions derived by using the MFE equation system. We have also combined the POD bases with a Galerkin projection procedure, thus yielding a new reduced model of lower dimensional order and of high accuracy for the tropical Pacific Ocean reduced gravity model. We have then proceeded to derive error estimates between our reduced format approximate solutions and the usual full order MFE numerical solutions, and have shown using numerical examples that the error between the POD approximate solution of reduced format and the full MFE solution is consistent with the theoretical error results obtained, thus validating both feasibility and efficiency of our reduced format. Future work in this area will aim to extend the reduced format, implementing it to a realistic sea forecast system and to more complicated PDEs, for instance, the nonlinear shallow water equation system consisting of water dynamics equations, silt transport equation and the equation of bottom topography change. We have shown both by theoretical analysis as well as by numerical examples that the reduced format presented herein has extensive perspective applications.

#### Acknowledgments

Z. Luo and J. Zhu acknowledge the support of the National Science Foundation of China Nos. 10471100 and 40437017, and Beijing Jiaotong University Science Technology Foundation. I.M. Navon acknowledges support of NSF Grant No. ATM-0201808.

<sup>1</sup> For interpretation of the references to colour in Fig. 2, the reader is referred to the web version of this article.

**Appendix A**

The proof of Theorem 1 is as follows.

Subtracting Problem (IV) and (3.7) from Problem (III) and (3.6) yields the following error equations:

$$\begin{aligned} \beta_r^u(t_s) - kf \sum_{j=M_1+1}^n \beta_j^v(t_s)(\Phi_j^v, \Phi_r^u) - kg' \sum_{l=M_2+1}^n \beta_l^h(t_s)(\Phi_l^h, \Phi_{rx}^u) \\ + kA \sum_{i=M_1+1}^n \beta_i^u(t_s)(\nabla \Phi_i^u, \nabla \Phi_r^u) = k(f_1^s, \Phi_r^u) + \beta_r^u(t_{s-1}), \\ r = M_1 + 1, M_1 + 2, \dots, n, \quad s = 1, 2, \dots, \end{aligned} \tag{A.1}$$

$$\begin{aligned} \beta_r^v(t_s) + kf \sum_{i=M_1+1}^n \beta_i^u(t_s)(\Phi_i^u, \Phi_r^v) - kg' \sum_{l=M_2+1}^n \beta_l^h(t_s)(\Phi_l^h, \Phi_{ry}^v) \\ + kA \sum_{j=M_1+1}^n \beta_j^v(t_s)(\nabla \Phi_j^v, \nabla \Phi_r^v) = k(f_2^s, \Phi_r^v) + \beta_r^v(t_{s-1}), \\ r = M_1 + 1, M_1 + 2, \dots, n, \quad s = 1, 2, \dots, \end{aligned} \tag{A.2}$$

$$\begin{aligned} \beta_\ell^h(t_s) + kH \sum_{i=M_1+1}^n \beta_i^u(t_s)(\Phi_{ix}^u, \Phi_\ell^h) \\ + kH \sum_{j=M_1+1}^n \beta_j^v(t_s)(\Phi_{jy}^v, \Phi_\ell^h) = \beta_\ell^h(t_{s-1}), \\ \ell = M_2 + 1, M_2 + 2, \dots, n, \quad s = 1, 2, \dots, \end{aligned} \tag{A.3}$$

along with the initial condition

$$\begin{aligned} \beta_r^u(0) &= (u(x, y, 0) - \bar{u}(x, y), \Phi_r^u(x, y)), \\ r &= M_1 + 1, M_1 + 2, \dots, n, \\ \beta_r^v(0) &= (v(x, y, 0) - \bar{v}(x, y), \Phi_r^v(x, y)), \\ r &= M_1 + 1, M_1 + 2, \dots, n, \\ \beta_\ell^h(0) &= (h(x, y, 0) - \bar{h}(x, y), \Phi_\ell^h(x, y)), \\ \ell &= M_2 + 1, M_2 + 2, \dots, n. \end{aligned}$$

Eqs. (A.1)–(A.3) can be written as in the following vector format:

$$\begin{aligned} \begin{pmatrix} \beta_u^s \\ \beta_v^s \\ \beta_h^s \end{pmatrix} = k \begin{pmatrix} -AD_1 & fB & g'C_1 \\ -fB^T & -AD_2 & g'C_2 \\ -HC_1^T & -HC_2^T & \mathbf{O} \end{pmatrix} \begin{pmatrix} \beta_u^s \\ \beta_v^s \\ \beta_h^s \end{pmatrix} \\ + k \begin{pmatrix} F_1^s \\ F_2^s \\ \mathbf{0} \end{pmatrix} + \begin{pmatrix} \beta_u^{s-1} \\ \beta_v^{s-1} \\ \beta_h^{s-1} \end{pmatrix}, \end{aligned} \tag{A.4}$$

where  $\mathbf{O}$  is a  $(n - M_2) \times (n - M_2)$  zero matrix,  $\mathbf{0}$  is a  $(n - M_2)$ -dimensional zero vector, and

$$\begin{aligned} D_1 &= \int_{\Omega} (\nabla \Phi_{M_1+1}^u, \dots, \nabla \Phi_n^u)^T (\nabla \Phi_{M_1+1}^u, \dots, \nabla \Phi_n^u) dx dy, \\ D_2 &= \int_{\Omega} (\nabla \Phi_{M_1+1}^v, \dots, \nabla \Phi_n^v)^T (\nabla \Phi_{M_1+1}^v, \dots, \nabla \Phi_n^v) dx dy, \\ C_1 &= \int_{\Omega} (\Phi_{M_2+1}^h, \dots, \Phi_n^h)^T ((\Phi_{M_1+1}^u)_x, \dots, (\Phi_n^u)_x) dx dy, \\ C_2 &= \int_{\Omega} (\Phi_{M_2+1}^h, \dots, \Phi_n^h)^T ((\Phi_{M_1+1}^v)_y, \dots, (\Phi_n^v)_y) dx dy, \\ B &= \int_{\Omega} (\Phi_{M_1+1}^v, \dots, \Phi_n^v)^T (\Phi_{M_1+1}^u, \dots, \Phi_n^u) dx dy, \\ F_1^s &= ((f_1^s, \Phi_{M_1+1}^u), \dots, (f_1^s, \Phi_n^u))^T, \\ F_2^s &= ((f_2^s, \Phi_{M_1+1}^v), \dots, (f_2^s, \Phi_n^v))^T, \\ \beta_u^s &= (\beta_{M_1+1}^u(t_s), \dots, \beta_n^u(t_s))^T, \\ \beta_v^s &= (\beta_{M_1+1}^v(t_s), \dots, \beta_n^v(t_s))^T, \\ \beta_h^s &= (\beta_{M_2+1}^h(t_s), \dots, \beta_n^h(t_s))^T. \end{aligned}$$

Since it is well known (see [9]) that

$$\begin{aligned} \|(\Phi_1^w, \dots, \Phi_{M_\kappa}^w, \Phi_{M_\kappa+1}^w, \dots, \Phi_n^w) - (0, \dots, 0, \Phi_{M_\kappa+1}^w, \dots, \Phi_n^w)\|_0^2 \\ = \sum_{i=M_\kappa+1}^n \lambda_i^w, \quad w = u, v, h; \quad \kappa = 1, 2, \end{aligned} \tag{A.5}$$

we obtain

$$\begin{aligned} \left\| (u_h^s - u_{M_1}^s, v_h^s - v_{M_1}^s, h_h^s - h_{M_2}^s) \right\|_0 \\ \leq \left\| (\beta_u^s, \beta_v^s, \beta_h^s)^T \right\| \left( \sum_{i=M_1+1}^n (\lambda_i^u + \lambda_i^v) + \sum_{i=M_2+1}^n \lambda_i^h \right)^{1/2}, \\ s = 1, 2, \dots, \end{aligned} \tag{A.6}$$

where  $\|\cdot\|$  is the norm of matrices or vector. From the inverse inequality (see [28] or [29]) and matrix normal property, we obtain

$$\begin{aligned} \|C_1\| &\leq \left\| (\Phi_{M_2+1}^h, \dots, \Phi_n^h)^T \right\|_0 \left\| (\Phi_{M_1+1}^u, \dots, \Phi_n^u)_x \right\|_0 \\ &\leq c\bar{h}^{-1} \left\| (\Phi_{M_2+1}^h, \dots, \Phi_n^h)^T \right\|_0 \left\| (\Phi_{M_1+1}^u, \dots, \Phi_n^u) \right\|_0 \\ &\leq c\bar{h}^{-1} \left( \sum_{i=M_1+1}^n \lambda_i^u \sum_{i=M_2+1}^n \lambda_i^h \right)^{1/2}, \end{aligned} \tag{A.7}$$

$$\|C_2\| \leq c\bar{h}^{-1} \left( \sum_{i=M_1+1}^n \lambda_i^v \sum_{i=M_2+1}^n \lambda_i^h \right)^{1/2}, \tag{A.8}$$

$$\|B\| \leq \left\| (\Phi_{M_1+1}^v, \dots, \Phi_n^v)^T \right\|_0 \left\| (\Phi_{M_1+1}^u, \dots, \Phi_n^u) \right\|_0 \left( \sum_{i=M_1+1}^n \lambda_i^u \sum_{i=M_1+1}^n \lambda_i^v \right)^{1/2}, \tag{A.9}$$

$$\begin{aligned} \|F_1^s\| &\leq \|f_1^s\|_0 \left\| (\Phi_{M_1+1}^u, \dots, \Phi_n^u) \right\|_0 \\ &= \|f_1^s\|_0 \left( \sum_{i=M_1+1}^n \lambda_i^u \right)^{1/2}, \end{aligned} \tag{A.10}$$

$$\begin{aligned} \|F_2^s\| &\leq \|f_2^s\|_0 \left\| (\Phi_{M_1+1}^v, \dots, \Phi_n^v) \right\|_0 \\ &= \|f_2^s\|_0 \left( \sum_{i=M_1+1}^n \lambda_i^v \right)^{1/2}. \end{aligned} \tag{A.11}$$

Then, multiplying (A.4) by  $((\beta_u^s)^T, (\beta_v^s)^T, (\beta_h^s)^T)$ , one could get

$$\begin{aligned} \begin{pmatrix} \beta_u^s \\ \beta_v^s \\ \beta_h^s \end{pmatrix}^T \begin{pmatrix} \beta_u^s \\ \beta_v^s \\ \beta_h^s \end{pmatrix} &= k \begin{pmatrix} \beta_u^s \\ \beta_v^s \\ \beta_h^s \end{pmatrix}^T \begin{pmatrix} -AD_1 & fB & g^T C_1 \\ -fB^T & -AD_2 & g^T C_2 \\ -HC_1^T & -HC_2^T & \mathbf{0} \end{pmatrix} \begin{pmatrix} \beta_u^s \\ \beta_v^s \\ \beta_h^s \end{pmatrix} \\ &+ k \begin{pmatrix} \beta_u^s \\ \beta_v^s \\ \beta_h^s \end{pmatrix}^T \begin{pmatrix} F_1^s \\ F_2^s \\ \mathbf{0} \end{pmatrix} + \begin{pmatrix} \beta_u^s \\ \beta_v^s \\ \beta_h^s \end{pmatrix}^T \begin{pmatrix} \beta_u^{s-1} \\ \beta_v^{s-1} \\ \beta_h^{s-1} \end{pmatrix}. \end{aligned} \tag{A.12}$$

Noting that  $A(\beta_u^s)^T D_1 \beta_u^s > 0$  and  $A(\beta_v^s)^T D_2 \beta_v^s > 0$ , if

$$\max \left\{ \left( \sum_{i=M_1+1}^n \lambda_i^u \right)^{1/2}, \left( \sum_{i=M_1+1}^n \lambda_i^v \right)^{1/2} \right\} \leq h/c,$$

which is reasonable, by using matrix normal property, and (A.4) and (A.7)–(A.12), one can obtain

$$\begin{aligned} \|(\beta_u^s, \beta_v^s, \beta_h^s)^T\| &\leq c_0 k \|(\beta_u^s, \beta_v^s, \beta_h^s)^T\| + C_0^s k \\ &+ \|(\beta_u^{s-1}, \beta_v^{s-1}, \beta_h^{s-1})^T\|, \end{aligned} \tag{A.13}$$

where

$$\begin{aligned} c_0 &= 2f \left( \sum_{i=M_1+1}^n \lambda_i^u \sum_{i=M_1+1}^n \lambda_i^v \right)^{1/2} + 2g' \left( \sum_{i=M_2+1}^n \lambda_i^h \right)^{1/2} \\ &+ 2H \left( \sum_{i=M_2+1}^n \lambda_i^h \right)^{1/2}, \end{aligned}$$

and

$$C_0^s = \|f_1^s\| \left( \sum_{i=M_1+1}^n \lambda_i^u \right)^{1/2} + \|f_2^s\| \left( \sum_{i=M_1+1}^n \lambda_i^v \right)^{1/2}.$$

Summing (A.13) from 1 to  $s$ , if  $k$  is sufficiently small, such that  $1 - c_0 k \leq 1/2$ , yields

$$\begin{aligned} \|(\beta_u^s, \beta_v^s, \beta_h^s)^T\| &\leq \bar{C}_2 \left( \sum_{i=M_1+1}^n \lambda_i^v \right)^{1/2} + \bar{C}_1 \left( \sum_{i=M_1+1}^n \lambda_i^u \right)^{1/2} \\ &+ c_0 k \sum_{i=0}^n \|(\beta_u^i, \beta_v^i, \beta_h^i)^T\| + \|(\beta_u^0, \beta_v^0, \beta_h^0)^T\|, \end{aligned} \tag{A.14}$$

where  $(\beta_u^0, \beta_v^0, \beta_h^0) = (\beta_{M_1+1}^u(0), \dots, \beta_n^u(0), \beta_{M_1+1}^v(0), \dots, \beta_n^v(0), \beta_{M_2+1}^h(0), \dots, \beta_n^h(0))$ ,  $\bar{C}_1 = 2k \sum_{i=0}^n \|f_1^i\|$ , and  $\bar{C}_2 = 2k \sum_{i=0}^n \|f_2^i\|$ . Noting that

$$\begin{aligned} \|(\beta_u^0, \beta_v^0, \beta_h^0)^T\| &\leq (\|u(x, y, 0)\|_0 + \|\bar{u}\|_0) \left\| (\Phi_{M_1+1}^u, \dots, \Phi_n^u) \right\|_0 \\ &+ (\|v(x, y, 0)\|_0 + \|\bar{v}\|_0) \left\| (\Phi_{M_1+1}^v, \dots, \Phi_n^v) \right\|_0 \\ &+ (\|h(x, y, 0)\|_0 + \|\bar{h}\|_0) \left\| (\Phi_{M_2+1}^h, \dots, \Phi_n^h) \right\|_0 \\ &\leq \bar{C}_3 \left[ \left( \sum_{i=M_1+1}^n \lambda_i^u \right)^{1/2} + \left( \sum_{i=M_1+1}^n \lambda_i^v \right)^{1/2} \right. \\ &\left. + \left( \sum_{i=M_2+1}^n \lambda_i^h \right)^{1/2} \right], \end{aligned} \tag{A.15}$$

where  $\bar{C}_3 = \max\{\|u(x, y, 0)\|_0 + \|\bar{u}\|_0, \|v(x, y, 0)\|_0 + \|\bar{v}\|_0, \|h(x, y, 0)\|_0 + \|\bar{h}\|_0\}$ . Using discrete Gronwall inequality for (A.14), one could obtain

$$\begin{aligned} \|(\beta_u^s, \beta_v^s, \beta_h^s)^T\| &\leq \bar{C}_4 \left[ \left( \sum_{i=M_1+1}^n \lambda_i^u \right)^{1/2} + \left( \sum_{i=M_1+1}^n \lambda_i^v \right)^{1/2} + \left( \sum_{i=M_2+1}^n \lambda_i^h \right)^{1/2} \right], \end{aligned} \tag{A.16}$$

where  $\bar{C}_4 = \exp(nkc_0) \max\{\bar{C}_1 + \bar{C}_3, \bar{C}_2 + \bar{C}_3, \bar{C}_3\}$ . Combining (A.6) with (A.16) and using Cauchy inequality yields Theorem 1.

### References

- [1] M.A. Cane, The response of an equatorial ocean to simple wind stress patterns. Part I. Model formulation and analytical results, *J. Mar. Res.* 37 (1979) 233–252.
- [2] R. Seager, S.E. Zebiak, M.A. Cane, A model of the tropical Pacific Sea surface temperature climatology, *J. Geophys. Res.* 93 (1988) 1265–1280.
- [3] L. Yu, J.J. O'Brien, Variational data assimilation for determining the seasonal net surface flux using a tropical Pacific Ocean model, *J. Phys. Oceanogr.* 5 (1995) 2319–2343.
- [4] K. Fukunaga, *Introduction to Statistical Recognition*, Academic Press, London, 1990.
- [5] I.T. Jolliffe, *Principal Component Analysis*, Springer, Berlin, 2002.
- [6] D.T. Crommelin, A.J. Majda, Strategies for model reduction: comparing different optimal bases, *J. Atmos. Sci.* 61 (2004) 2206–2217.
- [7] A.J. Majda, I. Timofeyev, E. Vanden-Eijnden, Systematic strategies for stochastic mode reduction in climate, *J. Atmos. Sci.* 60 (2003) 1705–1722.
- [8] F. Selten, Baroclinic empirical orthogonal functions as basis functions in an atmospheric model, *J. Atmos. Sci.* 54 (1997) 2100–2114.
- [9] P. Holmes, J.L. Lumley, G. Berkooz, *Turbulence, Coherent Structures, Dynamical Systems and Symmetry*, Cambridge University Press, Cambridge, 1996.
- [10] G. Berkooz, P. Holmes, J.L. Lumley, The proper orthogonal decomposition in analysis of turbulent flows, *Annu. Rev. Fluid Mech.* 25 (1993) 539–575.
- [11] W. Cazemier, R.W.C.P. Verstappen, A.E.P. Veldman, Proper orthogonal decomposition and low-dimensional models for driven cavity flows, *Phys. Fluid* 10 (1998) 1685–1699.
- [12] D. Ahlman, F. Serlund, J. Jackson et al., Proper orthogonal decomposition for time dependent lid-driven cavity flows, Research Report of Science Technology at University of Florida, 2005.

- [13] J.L. Lumley, Coherent structures in turbulence, in: R.E. Meyer (Ed.), *Transition and Turbulence*, Academic Press, London, 1981, pp. 215–242.
- [14] N. Aubry, P. Holmes, J.L. Lumley, et al., The dynamics of coherent structures in the wall region of a turbulent boundary layer, *J. Fluid Dyn.* 192 (1988) 115–173.
- [15] L. Sirovich, Turbulence and the dynamics of coherent structures. Parts I–III, *Q. Appl. Math.* 45 (3) (1987) 561–590.
- [16] R.D. Roslin, M.D. Gunzburger, R. Nicolaides, et al., A self-contained automated methodology for optimal flow control validated for transition delay, *AIAA J.* 35 (1997) 816–824.
- [17] H.V. Ly, H.T. Tran, Proper orthogonal decomposition for flow calculations and optimal control in a horizontal CVD reactor, Technical Report, CRSC-TR98-12 (Center for Research in Scientific Computation), North Carolina State University, 1998.
- [18] J. Ko, A.J. Kurdila, O.K. Redonitis et al., Synthetic jets, their reduced order modeling and applications to flow control, AIAA Paper number 99-1000, 37 Aerospace Sciences Meeting & Exhibit, Reno, 1999.
- [19] P. Moin, R.D. Moser, Characteristic-eddy decomposition of turbulence in channel, *J. Fluid Mech.* 200 (1989) 417–509.
- [20] M. Rajaei, S.K.F. Karlsson, L. Sirovich, Low dimensional description of free shear flow coherent structures and their dynamical behavior, *J. Fluid Mech.* 258 (1994) 1401–1402.
- [21] Y.H. Cao, J. Zhu, Z.D. Luo, I.M. Navon, Reduced order modeling of the upper tropical Pacific Ocean model using proper orthogonal decomposition, *Comput. Math. Appl.* 52 (2006) 1373–1386.
- [22] H.V. Ly, H.T. Tran, Proper orthogonal decomposition for flow calculations and optimal control in a horizontal CVD reactor, *Q. Appl. Math.* 60 (4) (2002) 631–656.
- [23] L. Sirovich, Turbulence and the dynamics of coherent structures. Parts I–III, *Q. Appl. Math.* XLV (3) (1987) 561–590.
- [24] R.A. Adams, *Sobolev Space*, Academic Press, New York, 1975.
- [25] Z.D. Luo, J. Zhu, Q.C. Zen, et al., Mixed finite element methods for the shallow water equations including current and silt sedimentation (I), the continuous-time case, *Appl. Math. Mech.* 25 (1) (2004) 80–92.
- [26] Z.D. Luo, J. Zhu, Q.C. Zen, et al., Mixed finite element methods for the shallow water equations including current and silt sedimentation (II), the discrete-time case along characteristics, *Appl. Math. Mech.* 25 (2) (2004) 186–202.
- [27] J. Stricherz, J.J. O'Brien, D.M. Legler, *Atlas of Florida State University Tropical Pacific Winds for TOGA 1966–1985*, Florida State University, Tallahassee, FL, 1992.
- [28] P.C. Ciarlet, *Finite Element Method for Elliptic Problems*, North-Holland, Amsterdam, 1978.
- [29] Z.D. Luo, *Mixed Finite Element Methods and Applications*, Chinese Science Press, Beijing, 2006.